

UNIVERSITY OF GRONINGEN

INDUSTRIAL INTERNSHIP

---

# Light scattering in nanocomposite lenses

---

*Author:*

Thijs TJEBBES (s4137043)

*Supervisors:*

Dr. T. TUKKER (ASML)

Prof. dr. R. HOEKSTRA (RUG)

## Abstract

It has been shown that diffractive optical elements can be replaced by a refractive doublet consisting of a nanocomposite and a glass. The major advantage of this is that the amount of stray light is strongly reduced. However, part of the light scatters on the nanoparticle inclusions in the nanocomposite, causing stray light none the less. This research focuses on finding the amount of scattering in an achromat of PMMA-TiO<sub>2</sub> nanocomposite and N-BK7. The concept of radiative transfer was used to model scattering in a plane parallel medium in MATLAB and this was compared to a Monte Carlo simulation of a large amount of rays in the same system. After verifying the validity of the Monte Carlo simulation, an achromat was designed, for which the amount of scattering could be calculated. The total intensity in the Monte Carlo model was around 18% more compared to the theoretical model, meaning more time needs to be invested in aligning the two models. The plane parallel medium caused around 1.2% of the light being scattered and the simulation of the achromat showed a halo of scattered light around the spot. This shows that in possible applications of nanocomposite achromats, such as complex lens designs, scattering causes a small, yet significant problem.

January 27, 2025

# 1 Introduction

This report summarizes the work of a 5 month internship at the Tech RES MET Optics & SXR Metrology department at ASML, during the final year of a master's degree in Applied Physics at the University of Groningen. This department is part of ASML Research, with the focus on metrology and optical design. The internship aimed at understanding light scattering within nanocomposite lenses, to provide a framework for possible applications, in specific the ones of interest to ASML. The internship is placed within the scope of a larger project, where ASML works together with the University of Eindhoven (TU/e).

In 2021 Markus Seesselberg and Daniel Werdehausen from Zeiss published a paper where they showed that diffractive optical elements (DOEs) can be replaced by a refractive doublet consisting of a nanocomposite material and a glass [1]. DOEs, for example Fresnel lenses, are lenses where the phase profile is folded, creating thin and micro-structured surfaces. The structure makes the lens useful for color correction in broadband optical systems, at the expense of a large amount of stray light. The paper shows that an achromat, consisting of a glass lens with an aspherical layer of a material with specific optical dispersion constants, can be used to reproduce the same broadband color correction as the structured lenses, without the large amount of stray light. However, the needed optical dispersion constants are not met by any of the regular lens materials, such as glasses, crystals and conventional polymers. The solution to this is to create a high refractive index material by dispersing high refractive index particles within a polymer. Using effective medium theory, it can be shown that this significantly changes the refractive index, creating the opportunity to engineer the optical dispersion. These nanocomposite materials provide promising specifications, but are still subject to some stray light, due to the scattering caused by the nanoparticle inclusions.

To understand scattering within nanocomposite materials, astrophysical models offer a good starting point. The physics behind light traveling through a layer of air in the atmosphere is similar to the physics behind light traveling through a nanocomposite material. Both consist of a medium filled with particles considerably smaller than the wavelengths of visible light. The problem definition is first simplified to light interacting with a single particle in an infinite medium, hereafter it is extended to many particles in a semi-infinite medium and lastly to many particles in a plane parallel medium. The last step is expected to offer results that closely resemble a nanocomposite lens.

These insights provide a benchmark that can be used to test whether simulation software yield the expected results. Since nanocomposite materials are not ordinary materials, it is important to verify the results using different methods. The goal of this research is to create a set of examples using theoretical models, that can be imitated in the simulation software, to validate that the correct boundary conditions are set. From there on, it is expected that the output of the simulation software provides results that follow the relevant physics, such that it can be used to model lenses from nanocomposite materials.

Two types of simulation software will be used, Ansys Zemax OpticStudio and LightTools. Zemax will be used to create an achromat, that is designed for in and out coupling in optical fibers. LightTools will be used to measure the amount of light scattering within this achromat. Before this can be done, the just sketched verification procedure will be followed. The LightTools simulation of the achromat gives an estimate of the amount of scattering, this can be used to design the appropriate experimental setup for measurements of the nanocomposite lenses, that are created by a PhD student of the TU/e.

## 2 Matlab model of light scattering

Scattering of electromagnetic waves, such as light, happens due to the heterogeneity of the system. All matter consists of discrete electric charges, electrons and protons, which are set in an oscillatory motion when illuminated by an electromagnetic wave. This acceleration of the electric charges radiates energy in all directions, which we know as the scattered radiation [2]. Theories that describe light traveling through heterogeneous environments can be used to model light scattering within nanocomposite materials, most of which are astrophysical models. In this chapter the complexity of the problem is gradually increased. First, the angular distribution of light scattering on a single particle in an infinite medium will be calculated. After which, the amount of particles is increased and the infinite medium is reduced to a semi-infinite medium and lastly it is further restricted to a plane parallel medium. An illustration of the three different cases can be seen in figure 1, which shows a large amount of nanoparticles in figures 1b and 1c to represent a nanocomposite. In reality, in 1 cm<sup>3</sup> of material, between 10<sup>22</sup> and 10<sup>24</sup> nanoparticles are dispersed. Despite this large number of particles, one can assume a maximum of one scatter event, due to the fact that the mean free path of the light is considerably larger than the thickness of the lenses.

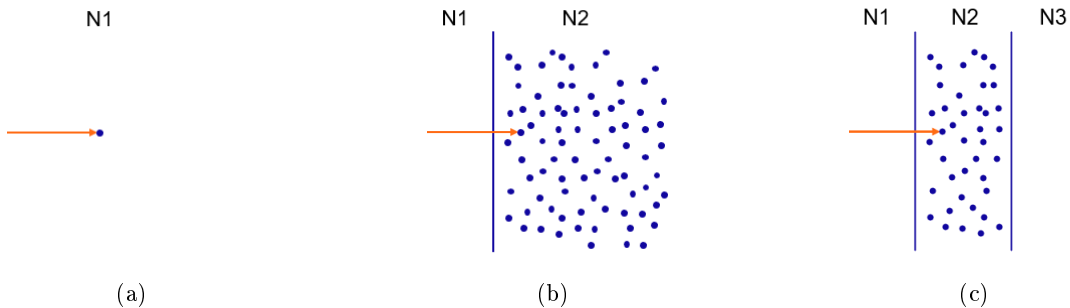


Figure 1: Schematic depiction of the different scenarios, ranging in order of complexity with in (a) the single particle in an infinite medium in (b) the semi-infinite medium and in (c) the plane parallel medium.  $n_1$ ,  $n_2$  and  $n_3$  are the refractive indices of the different media and the inclusions also have their individual refractive index.

### 2.1 Rayleigh and Mie

When a particle is illuminated by a beam of light the angular distribution of the scattered light and the absorption of the light in the material is dependent on the type of material, as well as on its size and shape [2]. Two scatter theories will be introduced, Rayleigh and Mie scattering, of which a typical angular scatter distribution is shown in figure 2. For round particles with sizes significantly smaller than the wavelength of the incident light, Rayleigh scattering can be used to approximate the angular distribution and the intensity of the scattered light. For round particles with larger sizes, Mie theory can be used. Mie theory is the exact solution to the Maxwell equations and returns to Rayleigh for smaller sizes, making it a more complete theory, at the cost of increased complexity. The main difference between the output of the theories is that in Rayleigh scattering forward and backward scattering are equal, while in Mie scattering forward scattering dominates. It was shown in [3] that the scattering amplitude for Rayleigh scattering  $\mathbf{f}(\hat{\mathbf{0}}, \hat{\mathbf{i}})$ , in the direction  $\hat{\mathbf{0}}$ , illuminated from direction  $\hat{\mathbf{i}}$ , is given by

$$\mathbf{f}(\hat{\mathbf{0}}, \hat{\mathbf{i}}) = \frac{k^2}{4\pi} \frac{3(\epsilon_r - 1)}{\epsilon_r + 2} V[-\hat{\mathbf{0}} \times (\hat{\mathbf{0}} \times \hat{\mathbf{e}}_i)], \quad (1)$$

where  $k$  is the wavenumber,  $\epsilon_r$  is the relative dielectric constant,  $V$  is the volume of the particle and  $\hat{\mathbf{e}}_i$

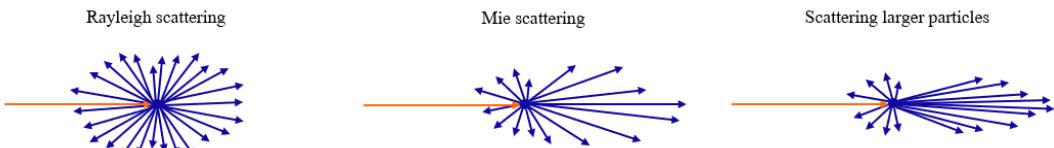


Figure 2: Difference in angular distribution between Rayleigh, Mie and larger particle scattering.

is the unit vector in the direction of the polarization of the light. Furthermore,  $||[-\hat{\mathbf{0}} \times (\hat{\mathbf{0}} \times \hat{\mathbf{e}}_i)]|| = \sin \chi$ , with  $\chi$  being the angle between  $\hat{\mathbf{e}}_i$  and  $\hat{\mathbf{0}}$ . Using equation (1), we can calculate the scattering cross section  $\sigma_s$ , which describes the probability of light scattering on the particle

$$\sigma_s = \int_{4\pi} |\mathbf{f}(\hat{\mathbf{0}}, \hat{\mathbf{i}})|^2 d\omega. \quad (2)$$

Furthermore, Ishimaru shows in [3] that we can calculate the absorption cross section, the probability of light being absorbed by the particle, using the imaginary part of the relative dielectric constant  $\epsilon_r''$

$$\sigma_a = k\epsilon_r'' \left| \frac{3}{\epsilon_r + 2} \right|^2 V. \quad (3)$$

Finally, the total cross section can be calculated by adding the scattering and absorption cross section

$$\sigma_t = \sigma_s + \sigma_a. \quad (4)$$

If we extend the problem to a large amount of particles in an infinite medium, we can calculate the mean free path of light through this infinite nanocomposite [4]

$$\frac{1}{\ell_t} = \rho\sigma_s(1 - \langle \cos \theta \rangle) + \rho\sigma_a, \quad (5)$$

where  $\rho$  is the density of the inclusions and  $\theta$  is the outgoing angle in which the intensity is measured. Applying these equations to nanocomposites ranging in volume fraction from 0 to 20% and in particle radius from 3 to 10 nm, it can be shown that the mean free path varies between 1 mm and 1 m. Since the nanocomposite lens will have a thickness around 100  $\mu\text{m}$ , the earlier stated assumption of 1 scatter event is valid.

Mie theory is the exact solution to the Maxwell equations for round, cylindrical and coated particles. Using the scattering coefficients  $a_n$  and  $b_n$ , given in [2], the scattering and total cross section can be calculated

$$\sigma_s = \frac{2\pi}{k^2} \sum_{n=1}^{\infty} (2n-1)(|a_n|^2 + |b_n|^2), \quad (6)$$

$$\sigma_t = \frac{2\pi}{k^2} \sum_{n=1}^{\infty} (2n-1) \operatorname{Re}\{a_n + b_n\}. \quad (7)$$

To calculate the shape of the angular distribution of the scattered light, the absolute value squared of the scattering functions  $S_1$  and  $S_2$  (see [2] for the derivation) describes the scattering intensities for perpendicular polarized light and parallel polarized light respectively. Mätzler created a MATLAB function that performs these calculations which was used to generate figure 3a [5]. In figure 3a, the top half of the sphere describes the scattered intensity of the perpendicular polarized light and the bottom half of the parallel polarized light. The left side, at  $\pi$  radians, describes backscattering and the right side, at 0 radians, the forward scattering. By comparing the intensities for these values the relative difference

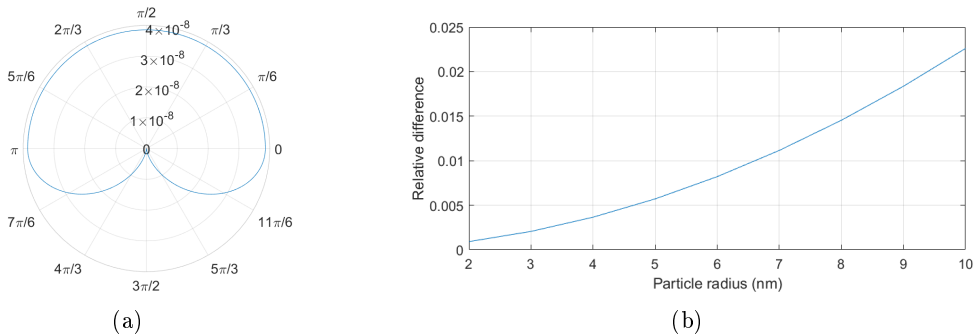


Figure 3: (a) Intensity of scattered light in polar coordinates, with perpendicular polarized light in the top half and parallel polarized light in the bottom half. (b) Relative difference between forward and backward scattering between Rayleigh and Mie scattering.

in forward and backward scattering can be calculated, as is shown in figure 3b. This relative difference is a measure of the deviation between Mie and Rayleigh. It can be seen that the forward scattering increases for increasing particle radius, as was also shown in figure 2. However, the relative difference between forward and backward scattering is negligible for the radii of interest for this research.

## 2.2 The Semi-infinite Medium

The scattering in the semi-infinite medium can be calculated using different approaches, of which the law of diffuse reflection is the most intuitive. The law of diffuse reflection calculates the diffuse intensity outside the medium using the concept of radiative transfer [6]. In this theory, only light that is scattered by the inclusions is taken into account and surface scattering is not included. The diffuse intensity is given by [3]

$$I_d = \frac{p(\mu, \phi; \mu_0, 0)}{4\pi} \left( \frac{\mu_0}{\mu_0 + \mu_r} \right) T_{12} T_{21} F_i, \quad (8)$$

where  $p$  is the phase function,  $\mu_0 = \cos(\theta_0)$  is the direction of the incident light,  $\mu_r = -\mu = -\cos(\theta)$  is the angle of reflection and  $T_{xy}$  is the transmission coefficient from medium  $x$  to medium  $y$  and is derived in [3]. The phase function represents the amount of scattered power and can be calculated in multiple different ways. For now, the phase function described by Rayleigh will be used, later the choice of the phase function will be discussed more elaborate

$$p(\mu, \phi; \mu_0, 0) = \frac{4\pi}{\sigma_t} |f(\mu, \phi; \mu_0, 0)|^2, \quad (9)$$

where  $\sigma_t$  is given by equation (4) and  $f(\mu, \phi; \mu_0, 0)$  by equation (1), with the incident and scattered direction given in polar coordinates.

The diffuse intensity versus the outgoing angle is shown in figure 4, both for the intensity of the scattered light within the material directly after the scatter incident and for the diffuse intensity outside the material. Snell's law is used to calculate this transition [3], which is shown in figure 4a. For light that is scattered under an angle that is larger than the described  $42^\circ$ , total internal reflection occurs and the light remains within the semi-infinite medium.

## 2.3 The Plane Parallel Medium

To make the transition from the semi-infinite medium to the plane parallel medium, an extra boundary has to be added where the refractive index of the material changes, placed at position  $d$ . In [3] it is shown that this leads to a diffuse intensity for  $z < 0$  and for  $z > d$ , given by

$$I_d^- = \frac{p(\mu, \varphi; \mu_0, 0)}{4\pi} \frac{\mu_0(1 - e^{\tau_0/\mu - \tau_0/\mu_0})}{\mu_0 - \mu} T_{12} F_0, \quad \text{for } -1 \leq \mu < 0 \quad (10)$$

$$I_d^+ = \frac{p(\mu, \varphi; \mu_0, 0)}{4\pi} \frac{\mu_0(e^{-\tau_0/\mu_0} - e^{-\tau_0/\mu})}{\mu_0 - \mu} T_{23} F_0, \quad \text{for } 0 < \mu \leq 1 \quad (11)$$

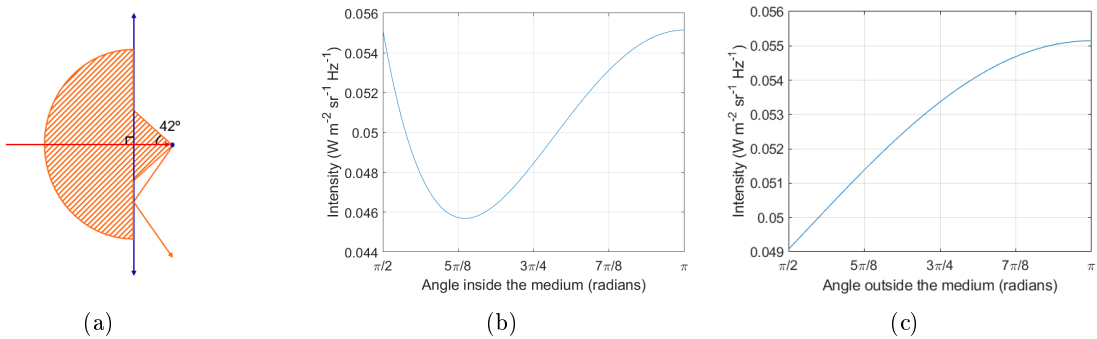


Figure 4: (a) A depiction of the range of angles under which the scattered light leaves the material as diffuse reflection and the intensity versus angle for (b) within the medium and (c) outside the medium.

where  $\tau = \rho\sigma_t z$  is the optical distance and  $\tau_0 = \rho\sigma_t d$ . As was also the case with the semi-infinite medium, Snell's law has to be taken into account when the diffuse intensity outside the medium is measured. Figure 5a shows that the light scattered within an angle of  $42^\circ$  leaves the medium, while the light scattered light at larger angles stays within the material due to total internal reflection. Furthermore, in some applications the light that leaves the medium in an angle over  $45^\circ$  can be blocked out. Figure 5b gives a presentation of this case, showing that only the light scattered within an angle of  $28^\circ$  is of interest.

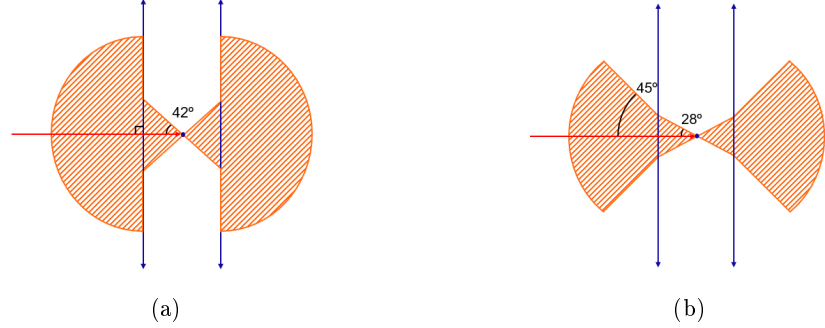


Figure 5: The difference between the angle after scattering and the angle when the light leaves the material, due to Snell's law for (a) all light leaving the material and (b) only the light that leaves the material at a maximum angle of  $45^\circ$  degrees.

Figure 6 shows the intensity versus angle outside the medium for both forward and backward scattering for the full range of angles and when the range of angles is limited to  $45^\circ$ . Forward scattering is at an angle of 0 radians and backward scattering at an angle of  $\pi$  radians. The total integrated diffuse intensity that is measured outside the plane parallel medium is  $0.012098I_i$ . The intensity reduces to  $0.0060329I_i$  for the  $45^\circ$  case, about half of the full diffuse intensity. The shape of the intensity curves show that the highest intensity occurs at the boundaries of the material and the lowest in the direction parallel to the beam. However, looking at the values it can be seen that they range between  $2.78 \times 10^{-3}$  and  $2.90 \times 10^{-3}$ , which shows the intensity is relatively constant over all angles.

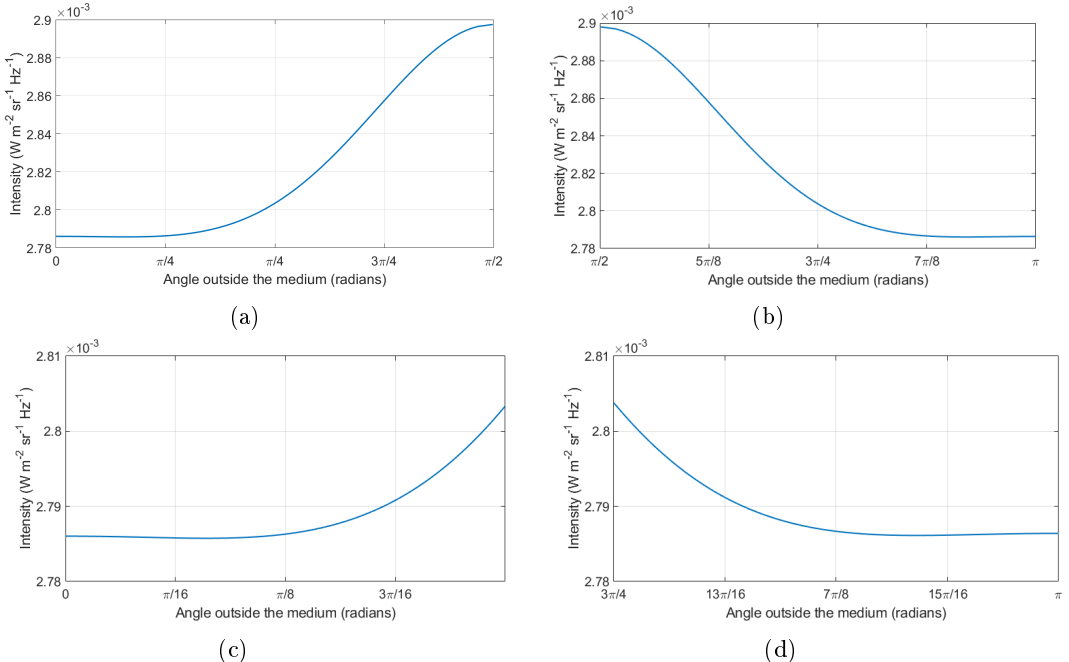


Figure 6: The diffuse intensity outside the medium for (a) all forward scattered light, (b) all backward scattered light, (c) forward scattered light under an angle of  $45^\circ$  degrees and (d) backward scattered light under an angle of  $45^\circ$  degrees.

### 3 Lens Design

For the design of optical systems Ansys Zemax OpticStudio (short Zemax) is used. This software can be used to model the interaction of light with various different optical elements. A wide variety of optimization factors are present to design an optical system with the desired specifications.

For this project, an achromat, consisting of an aspheric thin layer PMMA-TiO<sub>2</sub> nanocomposite and a relative thick layer N-BK7 is optimized for fiber in and out coupling. The nanocomposite is modelled using the effective medium theory Maxwell-Garnett Mie (which is extensively described in [7]), this provides a refractive index that lies somewhere between the refractive index of PMMA and that of TiO<sub>2</sub>. The lens is designed with a numerical aperture (NA) of 0.15. The detailed specifications and the numerical results will be left out, since this design is made using sensitive information. All images and values given in this chapter are fabricated, in order to give an insight in the process without giving away any information.

The design is optimized using three different wavelengths, the Fraunhofer F, d and C spectral lines. Since it is impossible to place a lens with absolute zero tilt, the lens should work according to specifications within the error range of the tilt, therefore three different fields, of which one is zero, are used. The light has a Gaussian distribution, with the peak at the center of the beam. The apodization factor, which is based on the NA of the lens and the NA of the fiber, determines how much the light at the edges is vignetted.

In the first optimization step, the focal shift between the F and the C line is set to zero, the effective focal length is set to the required value and the coma and spherical aberration are also set to zero. The optimization process is done using a couple parameters that can be varied. The radii of the front and back of the nanocomposite and the glass can be changed as well as the conic at the front of the nanocomposite layer. After this, only the requirement of the effective focal length is kept and the lens is optimized for minimal spot size using the same parameters. Last, higher order aspherical terms are added as parameters to the nanocomposite layer, while keeping an eye on the coupling efficiency. The higher order terms mostly provide a trade off between the fiber coupling efficiency for different wavelengths and fields. The amount of higher order terms is chosen such that the coupling efficiency is evenly spread. When the coupling efficiency is at its highest, while remaining constant over the different wavelengths and the different fields, the lens design is complete. Figure 7 shows an example of the final lens design, where it can be seen that the nanocomposite layer becomes thicker at the edges. Due to the Gaussian nature of the source, little light passes this part of the lens and the impact of this is minimal. The final lens design realized a coupling efficiency of 91% with a standard deviation over the different wavelengths and fields of 4.5%.

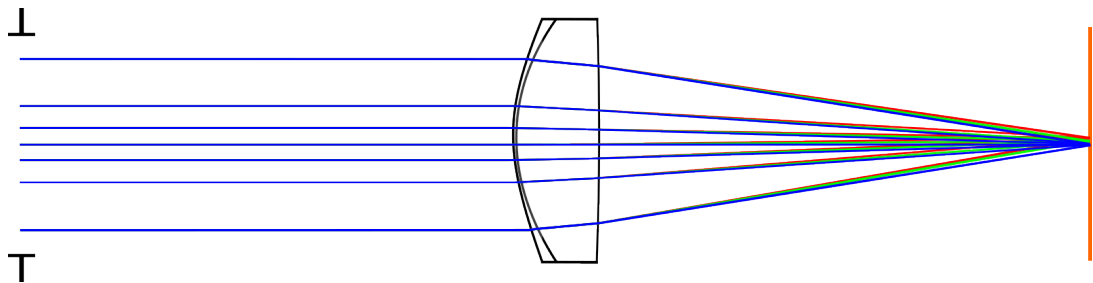


Figure 7: An illustration of the final lens design.

## 4 Monte Carlo Simulations

LightTools is an optical design and analysis software that uses the Monte Carlo method to ray trace a large amount of individual rays that can be used to simulate scattering. Because of the use of Monte Carlo simulations, far more complicated structures can be analyzed compared to Zemax, where the general interaction of light with a shape is of importance. By adding Mie particles to a medium, the amount of scattering in a nanocomposite can be simulated.

First, a plane parallel medium was created in LightTools by making a thin slab of nanocomposite material, that extends relatively far into the x and y directions. An example of this is shown in figure 8a, where the light source can be seen on the left, the slab is the nanocomposite and the semi-dome measures the specific intensity of the forward scattered light in  $\text{W mm}^{-2} \text{ sr}^{-1}$ . Figures 8b and 8c show specific intensity profiles created by simulating 100 million rays through the plane parallel nanocomposite. Since the theory states that the intensity is axial symmetric, it should not matter if the horizontal profile (along the x-axis in figure 8a) or the vertical profile (along the y-axis in figure 8a) is taken, both profiles are shown to verify this. The total specific intensity of the forward scattered light is  $0.003394I_i$  when the angles are limited to  $45^\circ$  and  $0.00715889I_i$  for the full range of angles. The intensity of the forward scattered light for the plane parallel medium described in section 2.3 is  $0.0030164I_i$  when the angles are limited to  $45^\circ$  and  $0.0060486I_i$  for the full range of angles.

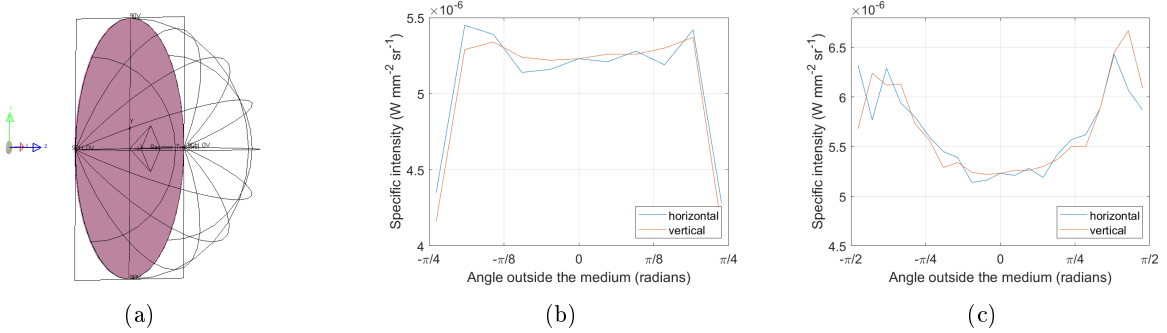


Figure 8: (a) Setup to measure the amount of specific intensity of scattered light in a plane parallel nanocomposite. (b) Horizontal and vertical intensity profile when the angles are limited to  $45^\circ$  and (c) when the full range of angles is measured.

Next, the lens shown in figure 7 is recreated in LightTools. The light is focused on a rectangular detector that represents an IMX290 sensor from SONY. The scattered light that lands on the detector creates noise around the unscattered light that carries the wanted information. To simulate the noise that would land on the sensor, only the light that experienced at least one scatter event is taken into account. Figure 9 shows the specific intensity map of the scattered light on the detector, using 10 million rays. It shows that the light is scattered evenly over the detector, which will create a halo of light around the unscattered signal.

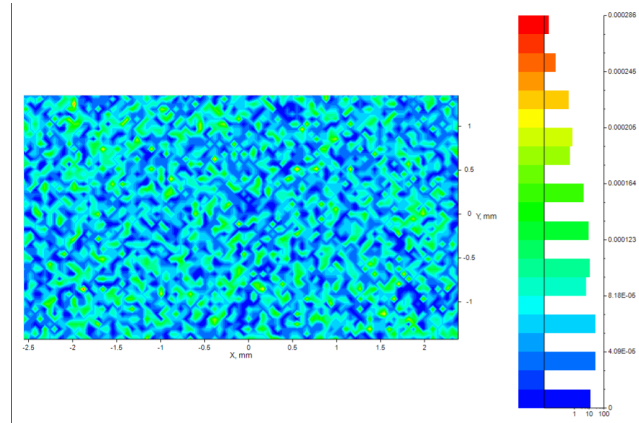


Figure 9: Intensity of the scattered light on an IMX290 sensor, after passing a doublet made out of a nanocomposite and N-BK7.

## 5 Discussion and Conclusion

The goal of this research was to find the amount of light that is scattered due to nanocomposite inclusions in an achromat of PMMA-TiO<sub>2</sub> nanocomposite and N-BK7. To achieve this the scattering within a plane parallel nanocomposite was modeled in MATLAB and compared to the same situation in LightTools. After the achromat was designed in Zemax, it could be implemented in LightTools to measure the total scattering on the sensor.

The intensity caused by the scattering in the plane parallel medium is measured in specific intensity ( $[W\ m^{-2}\ sr^{-1}\ Hz^{-1}]$ ). This unit represents the intensity from a specific direction with a specific wavelength and is not the same as intensity ( $[W\ m^{-2}]$ ). The difference between the two quantities caused some initial problems connecting the results of the simulation with the theory, since the specific intensity provides a completely different angular distribution. The specific wavelength is not relevant since the measurements are all performed at one specific wavelength (632.8 nm), however the direction is relevant. The theoretical model is incomplete since the intensity is relevant for the final result and it is not possible to describe it using this model. It was possible to compare the specific intensity in LightTools to the specific intensity found using the MATLAB model. Although this provides a first check on the similarity of the two models, it does not guarantee that the intensity found with the LightTools model is correct.

Figure 6 and figure 8 show the results of the MATLAB model and the LightTools simulation respectively. It can clearly be seen from the LightTools model that too little rays were used during this simulation. However, it was too computationally expensive to do larger simulations. Apart from this, the figures show that the vertical and horizontal data is very similar, as was expected since the intensity is axially symmetric. The shape of figure 8b and figures 6c and 6d are very similar and both tend to increase towards  $\pi/4$  and  $-\pi/4$ . The sudden drop in specific intensity at  $\pi/4$  and  $-\pi/4$  and in figure 8b can be explained by the bin sizes. However, the relative change between the middle and the edges is not the same. There is an increase in the specific intensity of around 3% for the LightTools model and an increase of around 0.7% for the MATLAB model. The values at the y-axis can not be directly compared since there is a difference in units between the two figures, but the difference in total forward intensity shows that the LightTools model predicts a 12.5% larger total specific intensity compared to the MATLAB model. Similar things can be seen when we compare figure 8c with figures 6a and 6b. The shape increases around the same point and stabilizes towards the edges in both cases, but the relative difference in intensities between the middle and the edges is about 10 times bigger for the LightTools model compared to the MATLAB model. The LightTools model predicts an 18% larger total specific intensity in the forward direction. The error on the LightTools measurements is 2%, due to the relatively low amount of rays. However, the signal to noise ratio increases with  $\sqrt{N}$ , meaning that a large amount of extra rays are needed to lower the error significantly. The differences between the Light tools model and the theoretical model are too significant to be explained by this error alone, meaning some other factor plays a role in this.

Figure 9 shows the scattered light incident on a sensor. This is only a small part of the scattered light, but for certain applications this noise has the greatest influence on the results. This simulation of 10 million rays shows a seemingly random distribution of the few scattered rays that fall on the sensor. The error on the data depicted in the figure amounts to 100%, which showcases that the amount of rays is too small to draw reliable conclusions. Nonetheless, looking at the data available it seems that a halo of light forms around the focused bundle.

The calculations of the specific intensity show that approximately 1.2 % of the light is scattered by the nanocomposite. However, the exact amount of scattered light has not yet been found and needs further research. The results of the LightTools and the MATLAB model are similar, but there is still a gap that needs to be bridged. An option would be to use Mie scattering instead of Rayleigh scattering to see if the assumption that the particles are small enough is valid. Furthermore, LightTools simulations of different particle radii can be done to check if there is a specific pattern or constant missing in one of the two models. Last, to validate the final LightTools model, the MATLAB model of the specific intensity must be expanded to include intensity as well. With this information the model of the achromat can be checked and it can be used to run more simulations.

## References

- (1) Seesselberg, M.; Werdehausen, D. In *International Optical Design Conference*, 2021, 120780K.
- (2) Bohren, C. F.; Huffman, D. R., *Absorption and scattering of light by small particles*; John Wiley & Sons: 2008.
- (3) Ishimaru, A. et al., *Wave propagation and scattering in random media*; Academic press New York: 1978; Vol. 2.
- (4) Meretska, M. L., *Taming a white LED*, 2018.
- (5) Mätzler, C., *MATLAB functions for Mie scattering and absorption, version 2*; Institute of Applied Physics, University of Bern: 2002.
- (6) Chandrasekhar, S., *Radiative Transfer*; Dover Books on Physics; Dover Publications: 2013.
- (7) Battie, Y; Resano-Garcia, A; Chaoui, N; Zhang, Y; En Naciri, A *The Journal of chemical physics* **2014**, 140.